Advances in Physics Theories and Applications
ISSN 2224-719X (Paper) ISSN 2225-0638 (Online)
Vol.89, 2025

Neutron Radiative Capture Cross Section Formula at Energies 30 keV and 1420 keV for Isotopes $_{20}Ca$,$_{22}Ti$,$_{30}Zn$,$_{32}Ge$,$_{33}As$,$_{34}Se$, and $_{36}Kr$

Mohammad Al Shaikh[1*] Dr. Abdullah Rastanawi[2] Dr. Solaiman Dibo[2]
Faculty of Since, University of AL-Baath Homs, Syria, PO Box 77, Homs, Syria
1. Master student in Department of Physics- Faculty of Science- Al-Baath University
2. Department of Physics- Faculty of Science- Al-Baath University
* E-mail of the corresponding author: Mohammad.alshaikh.mhcr7zzzzzzz@gmail.com

Abstract
In this research, we studied the effect of the number of protons and neutrons in the target nucleus on the cross-section of the radiative capture reaction to predict the nuclear parameters influencing the cross-section. These parameters vary with changes in the number of protons and neutrons in the target nucleus, exhibiting a behavior similar to the variation of the radiative capture cross-section values. We also aimed to find a relationship linking the cross-sections of the radiative capture reaction at energies of 30 keV and 1420 keV with the nuclear parameters of the isotopes $_{20}Ca$, $_{22}Ti$, $_{30}Zn$, $_{32}Ge$, $_{33}As$, $_{34}Se$, $_{36}Kr$.
Keywords: Radiation capture cross section, quadrupole deformation, Binding energy per nucleon, neutron separation energy
DOI: 10.7176/APTA/89-02
Publication date: August 31st 2025

1. Introduction

The reaction cross section is, by definition, the measure of the probability that a nuclear reaction will occur[1]،and the term reaction cross section is used, because it is a term that depicts the effective area of the target nucleus. It is not a measure of the true cross section of a target nucleus; rather, it is a measure of the effectiveness of the target nucleus to increase or reduce the probability of a nuclear reaction with a projectile particle[1]. While it is best to think of cross section as the probability of success, it is more strictly defined as the *apparent* cross-sectional area of the target nucleus as seen by the projectile[2]. Thus, its dimension is that of geometrical area. The cross section is not in general equal to the actual area of the nucleus[3]. The bottom line is that variations in nuclear cross sections are not as simple as comparing sizes of target nuclei. They sometimes vary wildly even for closely related target nuclides. For example, the thermal neutron cross section for the n, gamma reaction involving ^{1}H is 0.332 b but is 0.52 mb (*millibarns*) for ^{2}H [2].

This prompts us to study the factors related to nuclear structure that may influence the value of the cross-section and determine the methodology for these changes in its value.

2. The effect of the number of protons and neutrons on the cross-section.

In general, the cross-section of the radiative capture reaction increases with the increase in the number of protons and neutrons (mass number), as shown in Figures 1 and 2. These figures display the cross-sections of the radiative capture reaction, taken from the European Activation File EAF-2010 mentioned in reference [4], at energies of 30 keV and 1420 keV, as a function of the number of neutrons for the isotopes:$1 \leq Z \leq 100$

[1] The larger the reaction probability, the larger is the corresponding cross section.

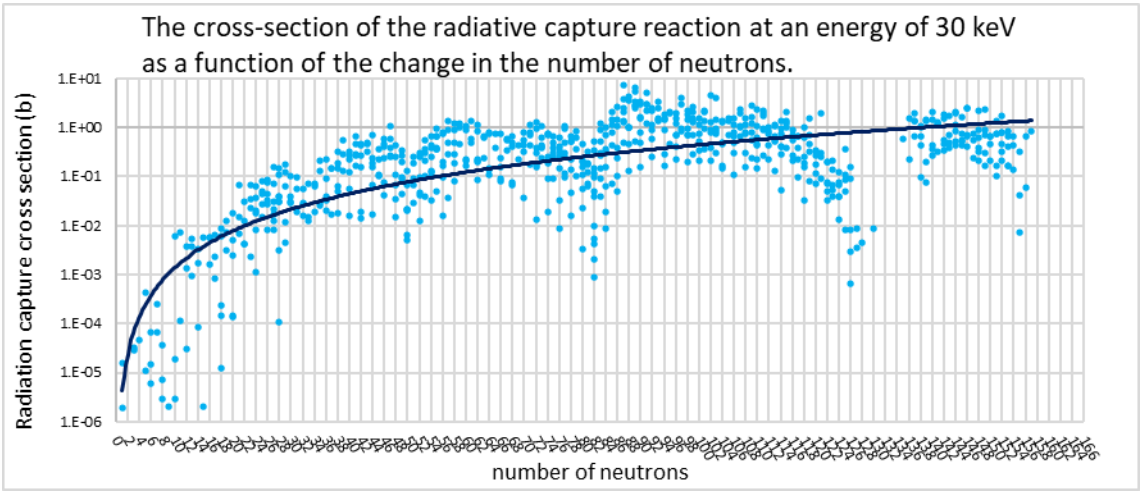

Figure 1. The cross-section of the radiative capture reaction at an energy of 30 keV as a function of the change in the number of neutrons.

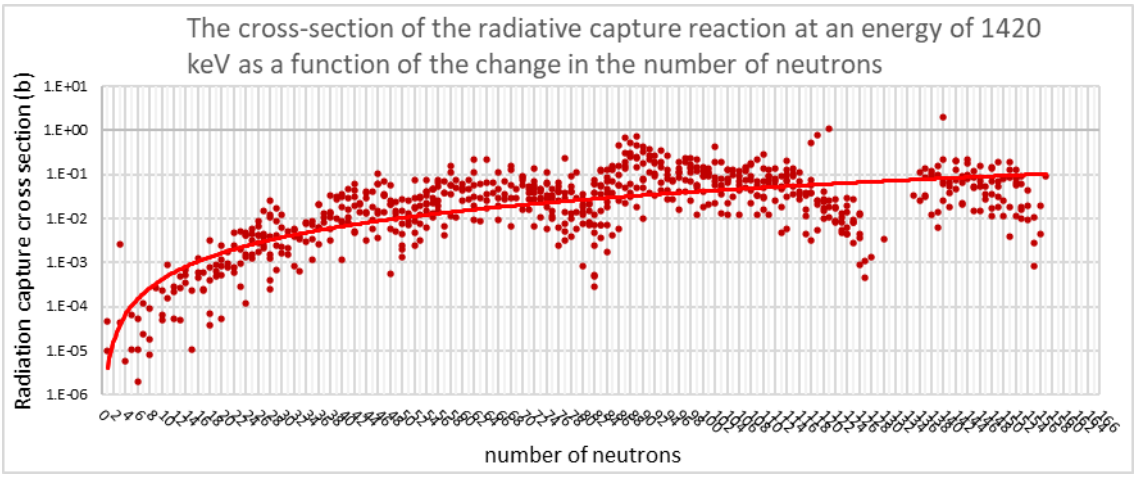

Figure 2. The cross-section of the radiative capture reaction at an energy of 1420 keV as a function of the change in the number of neutrons.

The cross sections are found to increase steadily as a function of the mass number up to a certain value at $A = 100$, after which there is no great change, with the marked exceptions of those nuclei for which there is a magic or near-magic number of protons or neutrons.

An increase in the mass number of the nucleus leads to:

1. An increase in the geometric radius of the target nucleus $R_t = r_0 A_t^{1/3}$, and the dependence of the cross-section on the radius RRR has been studied in references [5, 6].

$$\sigma_\gamma \propto R \quad (1)$$

2. An increase in the nuclear level density with the increase in mass number, as in the light nuclei, near the ground state, the levels are about 1 MeV apart, while in heavy nuclei about 50 keV apart, except in magic number nuclei [7]. The dependence of the radiative capture cross-section on the level density parameters a and excitation energy for the matching point U has been studied in references [8, 9].

$$\sigma_\gamma \propto aU \quad (2)$$

3. An increase in the number of scattering centers (nucleons) inside the nucleus leads to an increase in the number of interactions the neutron undergoes within the nucleus, and consequently:

$$\sigma_\gamma \propto (A + 1) \quad (3)$$

The values of the radiative capture cross-sections decrease at neutron numbers 8, 28, 50, 82, and 126. The gradient changes are sharp at the magic numbers and slow for the nuclides in between. The radiative capture cross-sections decrease with an increase in the number of neutrons for isotopes of the same element at energies of 30 keV and 1420 keV. The cross-sections of radiative capture are higher in isotopes with an odd number of neutrons. The cross-section values increase with the number of protons in isotonic chains.

4. The effect of the incoming neutron's wavelength on the cross-section.

The value of the radiative capture cross-section at an energy of 30 keV is often greater than at 1420 keV because:

1. Among neutrons passing close to a given nucleus, the slower neutrons spend more time near the nucleus and experience the nuclear forces for a longer time[10], which increases the probability of interactions.
2. Like any microscopic object, the neutron not only has a bodily aspect, but also a wave aspect. The wavelength associated with a neutron is calculated as follows:

$$\lambda(E) = \frac{h}{mv} = \frac{h}{\sqrt{2mE}} = \frac{2.86 \times 10^{-11}}{\sqrt{E}} \quad (4)$$

where λ is in m and E is in eV (non-relativistic De Broglie equation).
– in general, slow neutrons see a larger portion of space than fast neutrons, which means that slow neutrons often have larger cross-sections. More specifically, this also leads to the $1/v$ rule for absorption[11].
Consequently, the cross-section is directly proportional to the normalized wavelength $\lambda\!\!\!^{-} = \lambda/2\pi$.

$$\sigma_\gamma \propto \lambda\!\!\!^{-} \quad (5)$$

4. The effect of the binding energy of the neutron added to the target nucleus on the cross-section (neutron separation energy S_n from the compound nucleus in its ground state).
The nuclear analogs of atomic ionization energies are the "separation energies". The energy required to remove the least tightly bound neutron is called the *neutron separation energy* S_n [12]. Which equals to the binding energy of a neutron in a nucleus[7].
The one-neutron separation energies S_n are:

$$S_n = [m(^{A-1}_{Z}\mathrm{X}_{N-1}) + m_n - m(^{A}_{Z}\mathrm{X}_{N})]c^2 \quad (6)$$

$$S_n(Z,N) = E_b(Z,N) - E_b(Z,N-1) \quad (7)$$

These two quantities present discontinuities at special values of N or Z, which are called *magic numbers*[13].
S_n decreases with the increase of the neutron number for a given isotopic chain. S_n increases with the increase of the proton number for a given isotonic chain. Due to the pairing correlations, which make the nuclei with even nucleon number more bound than their neighbors with odd nucleon number, S_n has a ragged evolution pattern with the variation of neutron number that zigzags between odd- and even-particle nuclei[14].
The cross-sections of the radiative capture, taken from the European Activation File (EAF-2010) at energies of 30 keV and 1420 keV, were studied as a function of the neutron separation energy from the compound nucleus in its ground state, as mentioned in reference [14]. These predictions were made by the spherical relativistic continuum Hartree–Bogoliubov (RCHB) theory using the relativistic density functional PC-PK1, where by extending the relativistic mean field theory with the Bogoliubov transformation in the coordinate representation, the relativistic continuum Hartree– Bogoliubov (RCHB) theory was developed and it provides a proper treatment of pairing correlations and mean-field potentials in the presence of the continuum[14].
The radiative capture cross-sections increase with the increase in neutron separation energy S_n at energies of 30 keV and 1420 keV. Consequently, it is:

$$\sigma_\gamma \propto S_n \quad (8)$$

5. The effect of the average binding energy per nucleon in the target nucleus on the cross-section.
The energy required to separate a nucleus into individual nucleons is the *nuclear binding energy*. Nuclear binding energy could also be defined as the amount of energy released by the reverse process, that is, when a nucleus is assembled from its individual nucleons[2]. The binding energy B of a nucleus is defined as the negative of the difference between the nuclear mass and the sum of the masses of the constituents[13]:

$$B(A,Z) = Nm_nc^2 + Zm_pc^2 - m(A,Z)c^2 \quad (9)$$

Dividing the nuclear binding energy (or the mass defect) by the number of nucleons gives the average amount of energy it takes to pluck a single nucleon from that nucleus. In other words, how tightly held is each nucleon? This quantity is known as the *binding energy per nucleon.* Those nuclides with relatively high values for their binding energy per nucleon could be considered more stable than those with lower values[2].
slightly higher binding energies are observed in nuclei possessing a *magic number* of protons and/or neutrons: 8, 20, 28, 50, 82, or 126[11].
The effects of "asymmetry" and "pairing" also play an important role in determining the binding energy per nucleon, as predicted by the Weizsäcker mass formula [15].
The radiative capture cross-sections taken from the European Activation File (EAF-2010) at energies of 30 keV and 1420 keV were studied as a function of the experimental binding energy per nucleon in the target nucleus, as referenced in [14].
The cross-sections decrease with the increase in binding energy per nucleon for the studied isotopes of elements.
Consequently, the relationship is:

$$\sigma \propto \frac{1}{\left(\frac{B}{A}\right)} \quad (10)$$

6. The effect of the target nucleus deformation on the cross-section.

Nuclei with magic numbers of neutrons or protons have a "closed shell" that encourages a spherical shape. Nuclei with Z or N far from a magic number are generally deformed. The simplest deformations are so-called *quadrupole* deformations where the nucleus can take either a prolate shape (rugby ball) or oblate shape (cushion) [13]. The shape changes from spherical to deformed as more and more neutrons are added to the closed neutron core[16]. The quadrupole deformation β_2 calculated for the nuclear ground state is expressed using spherical harmonics expansion, as represented in equation (38) of the referenced publication[17].

$$\beta_{lm} = \sqrt{4\pi}\frac{\int r(\theta,\phi)Y_l^m(\theta,\phi)d\Omega}{\int r(\theta,\phi)Y_0^0(\theta,\phi)d\Omega}$$

The quadrupole deformation ($\beta_2 > 0$) is named "prolate" shape, while the quadrupole deformation ($\beta_2 < 0$) is called "oblate" shape[16].

The radiative capture cross-sections taken from the European Activation File (EAF-2010) at energies of 30 keV and 1420 keV were studied as a function of the absolute value of the quadrupole deformation parameter $|\beta_2|$ provided in reference [17]. This parameter was calculated for the nuclear ground state using the finite-range droplet model (FRDM), which is a hybrid macro-microscopic model for the mass formula, The FRDM is based on the macroscopic liquid drop model and takes into account the microscopic shell corrections[16].

The cross-sections increase with the increase in the quadrupole deformation parameter for the isotopes of the elements:

$$\sigma \propto |\beta_2| \tag{11}$$

7. Radiative capture cross-section formula.

In light of what has been studied in this research, we propose a relationship for the methodology of the radiative capture cross-section σ_γ(b) as a function of the following parameters:

- The normalized de Broglie wavelength of the incoming neutron λ(fm)
- The target nucleus radius R(fm) taken from reference [14]
- The number of nucleons in the compound nucleus $(A+1)$
- The neutron separation energy from the compound nucleus in its ground state S_n(MeV)
- The kinetic energy of the incoming neutron in the center-of-mass system $E_{n,c}$ (Note that the excitation energy gained by the compound nucleus is the sum of the binding energy of the incoming neutron (nuclear force work) and the kinetic energy provided by this neutron.)
- The binding energy per nucleon $\left({}^{B}/_{A}\right)$(MeV) in the target nucleus
- The absolute value of the quadrupole deformation parameter $|\beta_2|$
- The spin of the target nucleus in its ground state I_0 (where the spin of the target nucleus is one of the factors affecting the cross-section)

The relationship is given by:

$$\sigma_\gamma = c_1\pi(R+\lambda)^2(A+1)\left(\frac{(S_n+E_{n,c})}{\left({}^{B}/_{A}\right)}\right)^{n_1}(c_2|\beta_2|+1)^{n_2}(c_3I_0+1)^{n_3} \tag{12}$$

At energies of 30 keV and 1420 keV, through matching, we find that the parameters take the following values:

$$c_2 = 5\ ,\quad c_3 = 0.5,\quad n_2 = 5\ ,\quad n_1 = 1\ ,\quad n_3 = 1,$$

And c_1 varies for the studied isotopic chain according to the values in Table 1.

Table 1. Values of c_1 in formula (12) at energies of 30 keV and 1420 keV.

Isotopic chain for element	$c_{1(,30\ keV)}$	$c_{1,(1420\ keV)}$
${}_{20}Ca$	5.55×10^{-8}	5.51×10^{-8}
${}_{22}Ti$	3.83×10^{-8}	5.21×10^{-8}
${}_{30}Zn$	1.17×10^{-8}	1.87×10^{-8}
${}_{32}Ge$	0.50×10^{-8}	1.09×10^{-8}
${}_{33}As$	2.04×10^{-8}	0.94×10^{-8}
${}_{34}Se$	0.66×10^{-8}	1.76×10^{-8}
${}_{36}Kr$	1.86×10^{-8}	5.05×10^{-8}

Figure 3 shows a comparison of the values calculated using formula (12) with the values listed in the European Activation File (EAF 2010).

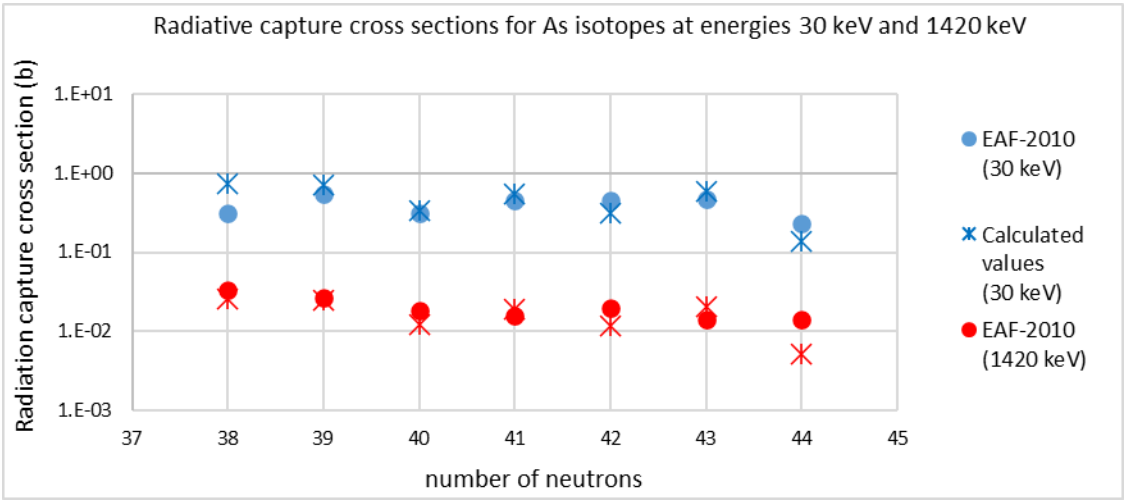

Figure 3. Comparison of the radiative capture cross-section values σ_γ calculated using formula (12) with the values listed in the European Activation File (EAF 2010) at energies of 30 keV and 1420 keV for the $_{33}$As isotopes.

Considering the effects of the level density parameter a and the excitation energy for the matching point U in the resulting compound nucleus, the methodology of the cross-sections takes the form:

$$\sigma_\gamma = c_1\pi(R+\lambda)^2(A+1)\left(\frac{(S_n+E_{n,c})}{(B/A)}\right)^{n_1}(c_2|\beta_2|+1)^{n_2}(c_3 I_0+1)^{n_3}(aU)^{n_4} \qquad (13)$$

The values of the level density parameters aU for the Gilbert-Cameron approach were adopted from the recommended values provided in the RIPL-2 report of 2006, as referenced in [18].

At energies of 30 keV and 1420 keV, through matching, we find that the parameters take the following values:

$$c_2 = 4\ , \quad c_3 = 0.5, \quad n_2 = 4\ , \quad n_1 = 0.5\ , \quad n_3 = 1, \quad n_4 = 1$$

And c_2 varies for the studied isotopic chain according to the values in Table 2.

Table 2. Values of c_1 in formula (13) at energies of 30 keV and 1420 keV.

Isotopic chain for element	$c_{1(,30\ keV)}$	$c_{1,(1420\ keV)}$
$_{20}Ca$	1.36×10^{-9}	2.5×10^{-9}
$_{22}Ti$	5.74×10^{-10}	2.32×10^{-9}
$_{30}Zn$	3.37×10^{-10}	7.58×10^{-10}
$_{32}Ge$	2.25×10^{-10}	5.75×10^{-10}
$_{34}Se$	6.31×10^{-10}	9.5×10^{-10}
$_{36}Kr$	9.81×10^{-10}	2.1×10^{-9}

Figure 4 shows a comparison of the values calculated using formula (13) with the values listed in EAF-2010 and ENDF/B-VII.1.

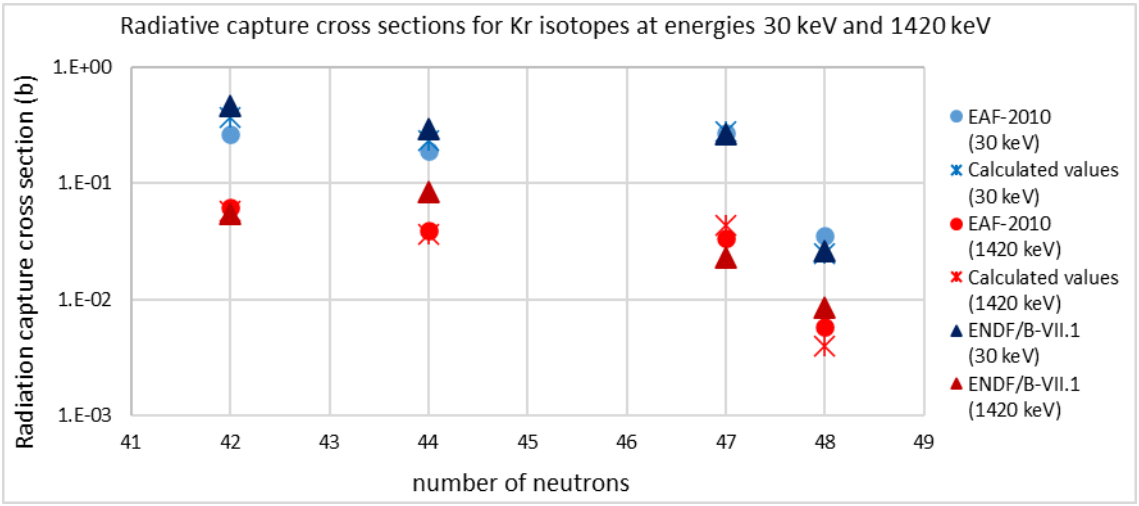

Figure 4. Comparison of the radiative capture cross-section values σ_γ calculated using formula (13) with the values listed in the European Activation File (EAF 2010) and ENDF/B-VII.1 at energies of 30 keV and 1420 keV for the $_{36}$Kr isotopes.

Taking into account the resonance parameters, average radiative widths Γ_γ, and average resonance spacings D_0, the methodology of the cross-sections takes the form:

$$\sigma_\gamma = c_1\pi(R+\lambda\!\!\!^{-})^2(A+1)\left(\frac{(S_n+E_{n,c})}{(B/A)}\right)^{n_1}(c_2|\beta_2|+1)^{n_2}(c_3I_0+1)^{n_3}(aU)^{n_4}\left(\frac{\Gamma_\gamma}{D_0}\right)^{n_5} \quad (14)$$

The values of $\frac{\Gamma_\gamma}{D_0}$ were adopted from the recommended values provided in the RIPL-2 report of 2006, as referenced in [18].

At energies of 30 keV and 1420 keV, through matching, we find that the parameters take the following values:

$c_2 = 4$, $c_3 = 0.5$, $n_2 = 4$, $n_1 = 0.5$, $n_3 = 0.5$, $n_4 = 0.25$, $n_5 = 0.25$

And c_1 varies for the studied isotopic chain according to the values in Table 3.

Table 3. Values of c_1 in relation (14) at energies of 30 keV and 1420 keV.

Isotopic chain for element	$c_{1(,30\ keV)}$	$c_{1,(1420\ keV)}$
$_{20}Ca$	3.16×10^{-7}	1.09×10^{-6}
$_{22}Ti$	2.74×10^{-7}	4.42×10^{-7}
$_{30}Zn$	7.74×10^{-8}	1.58×10^{-7}
$_{32}Ge$	6.55×10^{-8}	1.45×10^{-7}
$_{34}Se$	1.11×10^{-7}	2.05×10^{-7}

Figures 4, 5, 6, 7, and 8 show a comparison of the values calculated using formula (14) with the values listed in EAF-2010 and ENDF/B-VII.1.

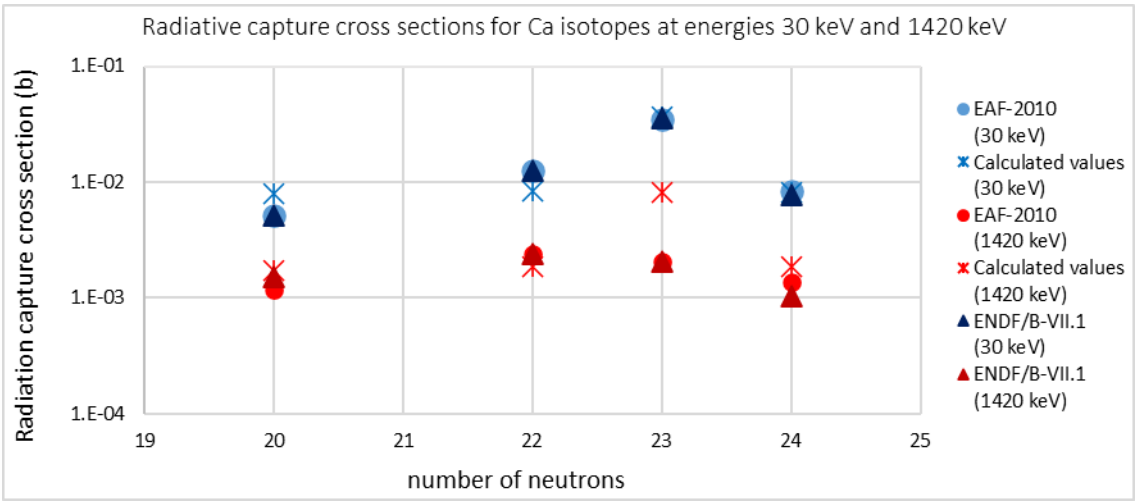

Figure 4. Comparison of the radiative capture cross-section values σ_γ calculated using formula (14) with the values listed in the European Activation File (EAF 2010) and ENDF/B-VII.1 at energies of 30 keV and 1420 keV for the $_{20}$Ca isotopes.

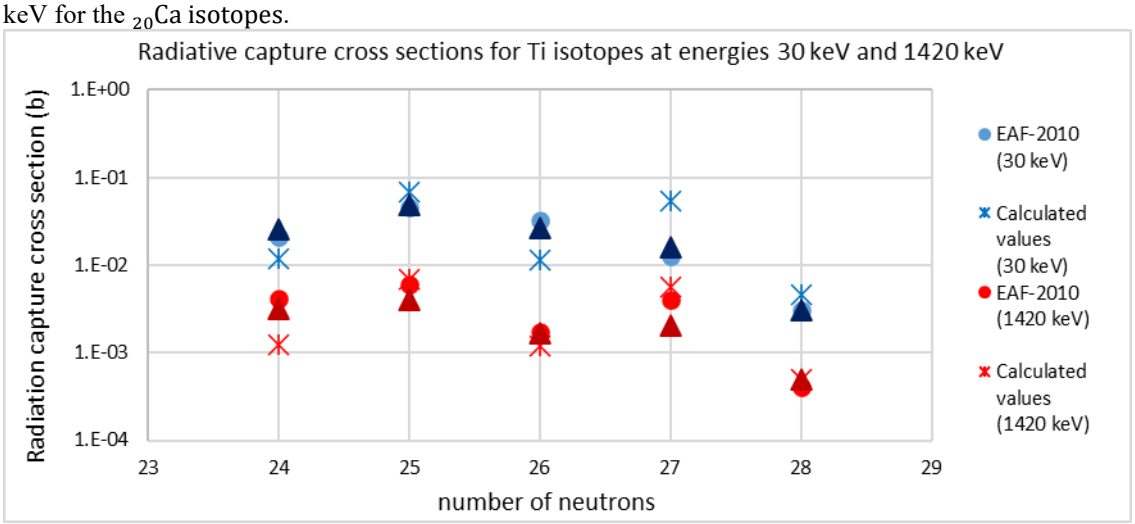

Figure 5. Comparison of the radiative capture cross-section values σ_γ calculated using formula (14) with the values listed in the European Activation File (EAF 2010) and ENDF/B-VII.1 at energies of 30 keV and 1420 keV for the $_{22}$Ti isotopes.

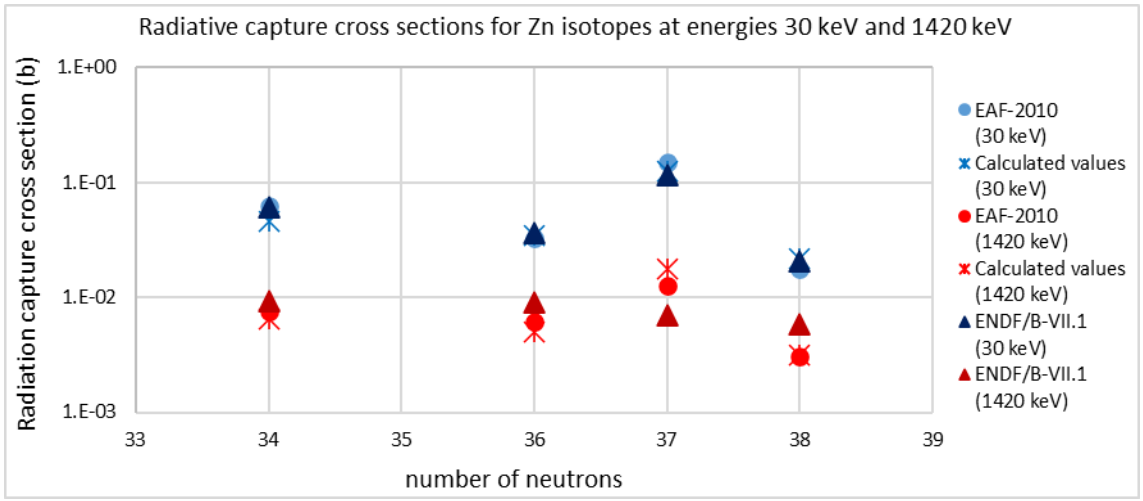

Figure 6. Comparison of the radiative capture cross-section values σ_γ calculated using formula (14) with the values listed in the European Activation File (EAF 2010) and ENDF/B-VII.1 at energies of 30 keV and 1420 keV for the $_{30}$Zn isotopes.

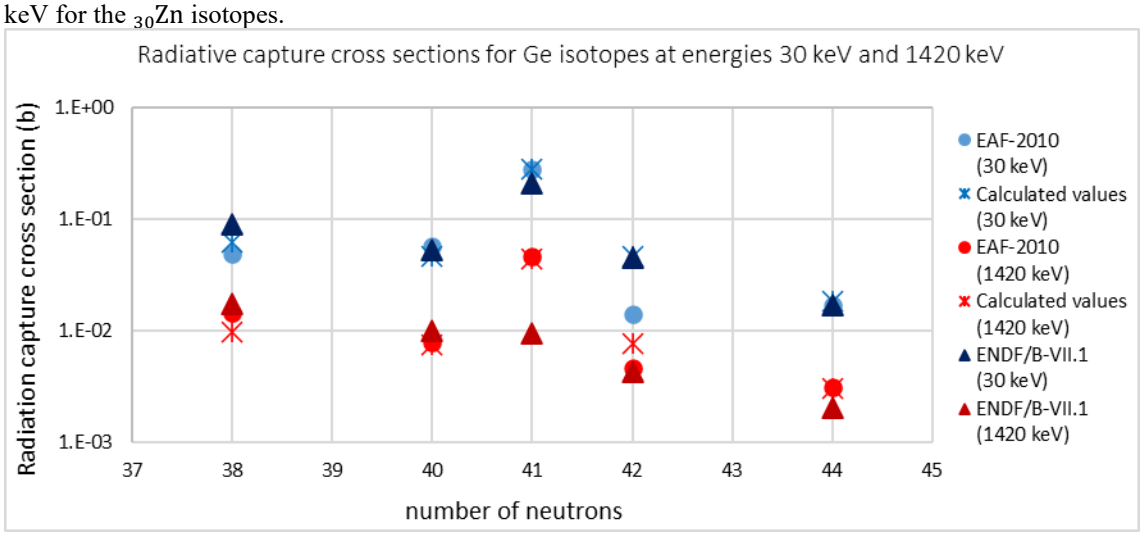

Figure 7. Comparison of the radiative capture cross-section values σ_γ calculated using formula (14) with the values listed in the European Activation File (EAF 2010) and ENDF/B-VII.1 at energies of 30 keV and 1420 keV for the $_{32}$Ge isotopes.

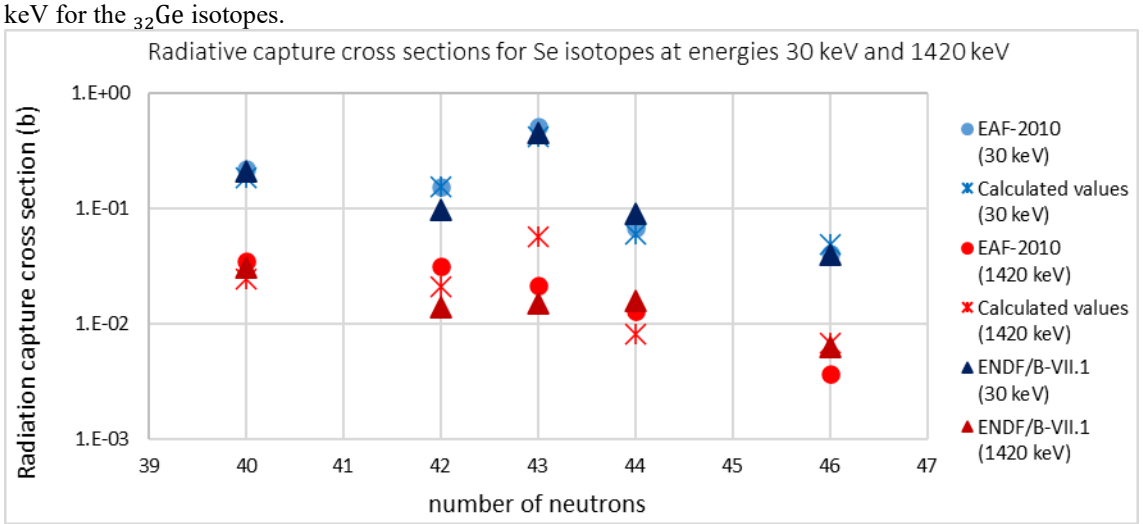

Figure 8. Comparison of the radiative capture cross-section values σ_γ calculated using formula (14) with the values listed in the European Activation File (EAF 2010) and ENDF/B-VII.1 at energies of 30 keV and 1420 keV for the $_{34}$Se isotopes.

Table 4 shows the values of the cross-sections calculated using formulas (12), (13), and (14), as well as the values listed in EAF-2010 and ENDF/B-VII.1.

Table 4. the values of the cross-sections calculated using formulas (12), (13), and (14), as well as the values listed in EAF-2010 and ENDF/B-VII.1.

Z	N	EAF-2010 (30 keV)	EAF-2010 (1420 keV)	ENDF/B-VII.1 (30 keV)	ENDF/B-VII.1 (1420 keV)	Eq(12) (30 keV)	Eq(12) (1420 keV)	Eq(13) (30 keV)	Eq(13) (1420 keV)	Eq(14) (30 keV)	Eq(14) (1420 keV)
20-Ca											
	20	5.15E-03	1.17E-03	5.14E-03	1.51E-03	6.43E-03	4.34E-04	8.01E-03	9.33E-04	7.97E-03	1.74E-03
	21	1.50E-02	1.74E-03			4.19E-02	2.73E-03				
	22	1.24E-02	2.40E-03	1.24E-02	2.37E-03	5.85E-03	4.06E-04	8.44E-03	1.00E-03	8.31E-03	1.85E-03
	23	3.47E-02	2.05E-03	3.53E-02	2.04E-03	3.14E-02	2.09E-03	5.03E-02	5.85E-03	3.70E-02	8.07E-03
	24	8.27E-03	1.37E-03	7.74E-03	1.04E-03	5.52E-03	3.93E-04	8.18E-03	9.88E-04	8.17E-03	1.85E-03
	25	1.50E-02	1.28E-03			3.02E-02	2.04E-03				
	26	8.02E-03	2.80E-03	1.86E-03	4.96E-04	5.28E-03	3.85E-04				
	27	1.74E-02	3.78E-03			4.60E-02	3.17E-03				
	28	1.09E-04	2.47E-04	1.08E-04	2.66E-04	4.66E-03	3.54E-04				
22-Ti											
	22	4.17E-03	6.10E-04			5.39E-03	5.01E-04				
	23	6.92E-02	5.17E-03			5.42E-02	4.89E-03				
	24	2.08E-02	4.14E-03	2.54E-02	3.13E-03	8.47E-03	8.00E-04	5.89E-03	1.54E-03	1.18E-02	1.24E-03
	25	4.53E-02	5.94E-03	4.86E-02	4.01E-03	5.21E-02	4.77E-03	3.54E-02	9.14E-03	6.77E-02	6.98E-03
	26	3.30E-02	1.73E-03	2.65E-02	1.64E-03	6.55E-03	6.29E-04	5.31E-03	1.41E-03	1.12E-02	1.19E-03
	27	1.28E-02	3.99E-03	1.58E-02	2.02E-03	6.17E-02	5.72E-03	3.79E-02	9.89E-03	5.36E-02	5.59E-03
	28	3.11E-03	4.04E-04	3.04E-03	5.04E-04	3.85E-03	3.90E-04	2.90E-03	7.92E-04	4.54E-03	4.95E-04
30-Zn											
	32	5.70E-02	5.91E-03			6.59E-02	7.74E-03				
	34	6.23E-02	7.63E-03	6.10E-02	9.17E-03	5.66E-02	6.76E-03	4.35E-02	6.79E-03	4.59E-02	6.52E-03
	35	1.28E-01	8.69E-03	1.68E-01	1.05E-02	1.30E-01	1.50E-02				
	36	3.29E-02	6.14E-03	3.64E-02	9.13E-03	5.11E-02	6.17E-03	3.94E-02	6.22E-03	3.45E-02	4.94E-03
	37	1.49E-01	1.27E-02	1.16E-01	7.00E-03	1.53E-01	1.80E-02	1.39E-01	2.17E-02	1.24E-01	1.77E-02
	38	1.79E-02	3.09E-03	2.08E-02	5.79E-03	3.05E-02	3.72E-03	2.69E-02	4.28E-03	2.18E-02	3.16E-03
	40	1.65E-02	1.18E-03	1.17E-02	2.00E-03	1.63E-03	2.12E-04	3.68E-03	6.09E-04		
	42	1.96E-02	5.19E-03			1.93E-03	2.61E-04				
32-Ge											
	36	9.14E-02	2.02E-02			8.60E-02	1.38E-02				
	37	1.45E-01	1.09E-02			1.62E-01	2.54E-02				
	38	4.90E-02	1.44E-02	8.91E-02	1.77E-02	4.69E-02	7.58E-03	5.46E-02	9.85E-03	6.29E-02	9.88E-03
	39	1.31E-01	1.00E-02			5.74E-02	9.22E-03				
	40	5.82E-02	7.97E-03	5.30E-02	1.02E-02	3.41E-02	5.83E-03	4.43E-02	8.25E-03	4.67E-02	7.58E-03
	41	2.81E-01	4.64E-02	2.10E-01	9.55E-03	1.80E-01	2.95E-02	2.61E-01	4.76E-02	2.79E-01	4.44E-02
	42	1.41E-02	4.69E-03	4.54E-02	4.35E-03	4.00E-02	7.01E-03	4.72E-02	8.94E-03	4.67E-02	7.69E-03
	44	1.72E-02	3.12E-03	1.70E-02	2.05E-03	1.50E-02	2.67E-03	2.28E-02	4.36E-03	1.85E-02	3.09E-03
	45	1.10E-01	5.94E-03			7.08E-02	1.19E-02				

Z	N	EAF-2010 (30 keV)	EAF-2010 (1420 keV)	ENDF/B-VII.1 (30 keV)	ENDF/B-VII.1 (1420 keV)	Eq(12) (30 keV)	Eq(12) (1420 keV)	Eq(13) (30 keV)	Eq(13) (1420 keV)	Eq(14) (30 keV)	Eq(14) (1420 keV)
33-As											
	38	3.16E-01	3.31E-02			7.28E-01	2.55E-02				
	39	5.51E-01	2.66E-02			7.09E-01	2.47E-02				
	40	3.14E-01	1.86E-02			3.38E-01	1.24E-02				
	41	4.59E-01	1.57E-02			5.45E-01	1.93E-02				
	42	4.49E-01	1.99E-02			3.15E-01	1.19E-02				
	43	4.70E-01	1.43E-02			5.79E-01	2.08E-02				
	44	2.33E-01	1.41E-02			1.37E-01	5.25E-03				
34-Se											
	38	6.38E-02	1.05E-02			1.72E-01	3.43E-02				
	39	2.91E-01	3.20E-02			4.96E-01	9.84E-02				
	40	2.20E-01	3.45E-02	2.08E-01	3.07E-02	6.86E-02	1.43E-02	1.97E-01	2.16E-02	1.82E-01	2.45E-02
	41	1.62E-01	1.09E-02			2.13E-01	4.30E-02				
	42	1.55E-01	3.12E-02	9.57E-02	1.38E-02	7.21E-02	1.53E-02	1.96E-01	2.17E-02	1.55E-01	2.11E-02
	43	5.06E-01	2.12E-02	4.45E-01	1.51E-02	1.41E-01	2.89E-02	3.86E-01	4.20E-02	4.18E-01	5.59E-02
	44	6.72E-02	1.29E-02	9.06E-02	1.57E-02	2.82E-02	6.08E-03	9.01E-02	1.01E-02	5.90E-02	8.12E-03
	45	1.05E-01	9.34E-03	4.15E-01	1.91E-02	1.09E-01	2.24E-02				
	46	4.08E-02	3.63E-03	3.93E-02	6.35E-03	2.83E-02	6.19E-03	3.99E-02	4.50E-03	4.89E-02	6.78E-03
	48	1.51E-02	5.73E-04	3.11E-02	9.64E-03	2.10E-02	4.64E-03	3.47E-02	3.95E-03		
36-Kr											
	40	2.67E-01	3.06E-02			1.13E+00	2.37E-01				
	42	2.69E-01	6.24E-02	4.70E-01	5.50E-02	2.41E-01	5.14E-02	3.72E-01	5.83E-02		
	43	3.31E-01	2.30E-02			4.54E-01	9.38E-02				
	44	1.89E-01	3.91E-02	2.94E-01	8.51E-02	2.93E-01	6.33E-02	2.32E-01	3.67E-02		
	45	2.21E-01	1.87E-02			1.86E-01	3.89E-02				
	46	7.86E-02	1.45E-02	1.03E-01	2.62E-02	4.98E-02	1.09E-02				
	47	2.74E-01	3.42E-02	2.67E-01	2.32E-02	2.17E-01	4.57E-02	2.78E-01	4.37E-02		
	48	3.54E-02	5.74E-03	2.64E-02	8.56E-03	2.47E-02	5.44E-03	2.49E-02	3.99E-03		
	49	4.44E-02	4.94E-03	1.22E-01	2.01E-02	8.75E-02	1.86E-02				
	50	5.07E-03	1.31E-03	5.06E-03	1.31E-03	2.21E-03	5.56E-04				

8. Conclusion

Nuclear reactions are essential for obtaining information about nuclear structure from experiments. Understanding how nuclear structure affects the reaction cross-section is crucial for enhancing our comprehension of nuclear interactions and their practical applications. By clarifying the role of nuclear structure in neutron-induced reactions, researchers can improve the accuracy of nuclear models and simulations, leading to more efficient and reliable techniques.

In this research, we aimed to achieve a partial objective that could help researchers approach or facilitate the development of a general relationship for the cross-section that incorporates all influencing factors. Continued research into the factors affecting cross-section values, as predicted by modern nuclear models, is necessary to establish a general relationship that provides cross-section values across a broader range of energies.

Further research should focus on identifying additional influencing factors to establish a general formula that provides radiative capture cross-section values for all isotopic chains. This study could also be valuable for researchers in deriving partial cross-section relationships for other reactions, such as (n,p), (n,α), and (n,f),

among others. This can be achieved by enhancing the formula presented in this research with the parameters specific to the desired reaction.

References

[1]. L'Annunziata, M. F. (Ed.). (2020). *Handbook of radioactivity analysis Volume 1: Radiation Physics and Detectors*. Academic press. Fourth Edition.
[2]. Bryan, J. C. (2018). *Introduction to nuclear science*. CRC press. Third Edition.
[3]. Ragheb, M. (2011). Neutron cross sections. *University of Illinois*.
[4]. Pritychenko, B., & Mughabghab, S. F. (2012). Neutron thermal cross sections, Westcott factors, resonance integrals, Maxwellian averaged cross sections and astrophysical reaction rates calculated from the ENDF/B-VII. 1, JEFF-3.1. 2, JENDL-4.0, ROSFOND-2010, CENDL-3.1 and EAF-2010 evaluated data libraries. *Nuclear Data Sheets*, *113*(12), 3120-3144.
[5]. Krane, K. S. (1991). *Introductory nuclear physics*. John Wiley & Sons.
[6]. Satchler, G. R., & Satchler, G. R. (1990). *Introduction to nuclear reactions* (pp. 21-88). Palgrave Macmillan UK.
[7]. Kamal, A. (2014). *Nuclear physics*. Springer.
[8].Forrest, R. A., Kopecky, J., & Koning, A. J. (2008). Revisions and improvements of neutron capture cross sections for EAF-2009 and validation of TALYS calculations. *UKAEA report UKAEA FUS*, *546*.
[9]. Sublet, J. C., Packer, L. W., Kopecky, J., Forrest, R. A., Koning, A. J., & Rochman, D. A. (2010). The European Activation File: EAF-2010 neutron-induced cross section library. *EASY documentation series CCFE*.
[10]. Nielsen. J . (2019). *Principles and Practices of Engineering PE Nuclear Reference Handbook* .National Council of Examiners for Engineering and Surveying (NCEES).
[11]. Reuss, P. (2008). Neutron physics.
[12]. Krane, K. S. (2019). *Modern physics*. John Wiley & Sons.
[13].Basdevant, J. L., Rich, J., & Spiro, M. (2005). *Fundamentals in nuclear physics: From nuclear structure to cosmology*. Springer Science & Business Media.
[14]. Xia, X. W., Lim, Y., Zhao, P. W., Liang, H. Z., Qu, X. Y., Chen, Y., ... & Meng, J. (2018). The limits of the nuclear landscape explored by the relativistic continuum Hartree–Bogoliubov theory. *Atomic Data and Nuclear Data Tables*, *121*, 1-215.
[15]. NAPOLITANO, J. (2021). *Origins of Nuclear Energy. In: Encyclopedia of Nuclear Energy,* vol. 1, Elsevier, pp. 29–34.
[16]. Obertelli, A., & Sagawa, H. (2021). *Modern Nuclear Physics: From Fundamentals to Frontiers*. Springer Nature.
[17]. Möller, P., Sierk, A. J., Ichikawa, T., & Sagawa, H. (2016). Nuclear ground-state masses and deformations: FRDM (2012). *Atomic Data and Nuclear Data Tables*, *109*, 1-204.
[18]. Belgya, T., Bersillon, O., Capote, R., Fukahori, T., Zhigang, G., Goriely, S., ... & Young, P. G. (2006). Handbook for calculations of nuclear reaction data, RIPL-2 (Reference Input Parameter Library-2). In *IAEA-Tecdoc-1506*.